Magnetic ordering in copper oxide planes of non-superconducting $Bi_2Sr_2Ca_{0.3}Y_{0.7}Cu_{1.96}Fe_{0.04}O_{8.37}$

1993 J. Phys.: Condens. Matter 5 8897

(http://iopscience.iop.org/0953-8984/5/47/014)

J. Phys.: Condens. Matter 5 (1993) 8897–8904. Printed in the UK

Magnetic ordering in copper oxide planes of non-superconducting $Bi_2Sr_2Ca_{0.3}Y_{0.7}Cu_{1.96}Fe_{0.04}O_{8.37}$

C M Lin and S T Lin

Department of Physics, National Cheng Kung University, Tainan, Taiwan, Republic of China

Received 23 March 1993, in final form 26 July 1993

Abstract. The hyperfine interaction at ^{57}Fe nuclei in $Bi_2Sr_2Ca_{0.3}Y_{0.7}Cu_{1.96}{}^{57}Fe_{0.04}O_{8.37}$ was investigated by Mössbauer spectroscopy in the temperature range 4.2–417 K. Magnetic ordering was observed below the Néel temperature of about 412 ± 5 K. The temperature dependence of the magnetic hyperfine field at ^{57}Fe nuclei could be well described using a highly anisotropic three-dimensional antiferromagnetic model. The intra-planar exchange energy J and the ratio γ of effective inter-planar to planar hopping strength are determined to be 2728 K and 0.004, respectively, by fitting. The effective magnetic hyperfine field H at 4.2 K is 499 kOe.

1. Introduction

One of the common characteristics of high-T_c superconducting copper oxides is the presence of antiferromagnetic spin ordered states in their insulating regimes. Therefore, studies of the magnetic properties of their antiferromagnetic states have attracted considerable interest. La_2CuO_4 and $YBa_2Cu_3O_{7-\delta}$ with $\delta > 0.5$ are both antiferromagnetic insulators, and the temperature dependence of their sublattice magnetizations has already been determined by muon spin relaxation (μSR) [1–3], neutron diffraction [4–6], nuclear quadrupole resonance (NQR) [7] and Mössbauer effect [8–10] measurements. For La_2CuO_4, the magnetic ordering of Cu spins in CuO_2 planes can be described by an anisotropic three-dimensional antiferromagnetic model with very weak inter-planar coupling [8]. The antiferromagnetic ordering of Cu spins on CuO_2 planes in $YBa_2Cu_3O_{7-\delta}$ with $\delta > 0.5$ is strongly affected by a small number of 2p holes, but the antiferromagnetic state with no hole in the CuO_2 planes could be well described by a quasi-two-dimensional Heisenberg model with a small XY anisotropy [6]. For the 85 K superconductor $Bi_2Sr_2CaCu_2O_y$, the compound $Bi_2Sr_2Ca_{1-x}Y_xCu_2O_y$ with $x > 0.5$ is the corresponding antiferromagnetic insulating phase. In this paper, we determine the temperature dependence of the magnetization for $Bi_2Sr_2Ca_{0.3}Y_{0.7}Cu_{1.96}Fe_{0.04}O_{8.37}$ by means of Mössbauer spectroscopy and compare our results with theoretical models.

2. Experiment

The sample was prepared by solid state reaction to form the compound of a nominal composition $Bi_2Sr_2Ca_{0.3}Y_{0.7}Cu_{1.96}Fe_{0.04}O_y$. 99% pure powders of Bi_2O_3, $SrCO_3$, $CaCO_3$, CuO and Fe_2O_3 (93% enriched in ^{57}Fe) were thoroughly mixed and calcined in air at 820 °C for 2 h. The calcined powder was pulverized, pressed into a pallet and sintered at 900 °C for 5 d in air and then it was subsequently cooled in a furnace to room temperature.

0953-8984/93/478897+08$07.50

The x-ray powder diffraction measurement was carried out using Cu Kα radiation. Magnetic susceptibility measurements with a SQUID magnetometer were used to identify the minor phase $Y_2Cu_2O_5$ in the sample. The average oxygen content for $Bi_2Sr_2Ca_{0.3}Y_{0.7}Cu_{1.96}Fe_{0.04}O_y$ was determined by a chemical iodometry titration method. The influence of the $Y_2Cu_2O_5$ impurity and Fe atoms upon the measured oxygen content is ignored here. The Mössbauer equipment was of conventional transmission type with a radioactive source consisting of ^{57}Co in a Rh matrix. A liquid-helium flow cryostat and an electric furnace were used to obtain sample temperatures in the range 4.2–417 K. The vacuum in the furnace was kept below 2×10^{-5} Torr. The Mössbauer spectra were analysed using the least-squares fitting method.

3. Results and discussion

In the initial stage of our work, we found that the Néel temperature T_N of the as-prepared $Bi_2Sr_2Ca_{0.3}Y_{0.7}Cu_{1.96}Fe_{0.04}O_y$ determined by Mössbauer effect measurements slowly increases as the time for aging this sample in a chamber increases. The time dependence of T_N values was thought to arise from the desorption of oxygen atoms. Therefore we first found the relationship between the oxygen content, T_N and the time for the as-prepared sample aged at room temperature. The oxygen content of the sample as a function of aging time is listed in table 1. Oxygen desorption is seen to take place significantly at room temperature and the oxygen content y of the sample approaches 8.37 if the aging time is sufficiently long. We also annealed the as-prepared samples at different temperatures for 30 min under a vacuum of less than 2×10^{-5} Torr and then measured their oxygen contents and T_N-values. The results are presented in table 2. It is clearly seen that T_N increases with decreasing oxygen content. The above results indicate that the as-prepared sample is unstable and the increase in its T_N-value with increase in the aging time is indeed due to the desorption of oxygen atoms. Finally, we use the stable sample with $y = 8.37$ to perform the following measurements and this sample will be referred to as B2:2:1:2YF for convenience.

Table 1. The average oxygen contents for the as-prepared $Bi_2Sr_2Ca_{0.3}Y_{0.7}Cu_{1.96}Fe_{0.04}O_y$ after aging at room temperature for different times.

Sample aging time (d)	Average oxygen content y
As prepared	8.48
7	8.38
15	8.37
19	8.37

The x-ray powder diffraction pattern of B2:2:1:2YF is shown in figure 1(*b*). Its character is similar to that for $Bi_2Sr_2CaCu_2O_y$ (see figure 1(*a*)). No impurity phase in B2:2:1:2YF can be clearly identified from the x-ray diffractogram. However, from the temperature-dependent magnetic susceptibility of the sample shown in figure 2, a sharp cusp was found at around 10 K and this has been confirmed to originate from the existence of the minor second phase $Y_2Cu_2O_5$ [11, 12].

Mössbauer spectra of B2:2:1:2YF at some selected temperatures are plotted in figure 3. The full curves are the theoretical curves. Only the spectrum at 417 K is fitted with two

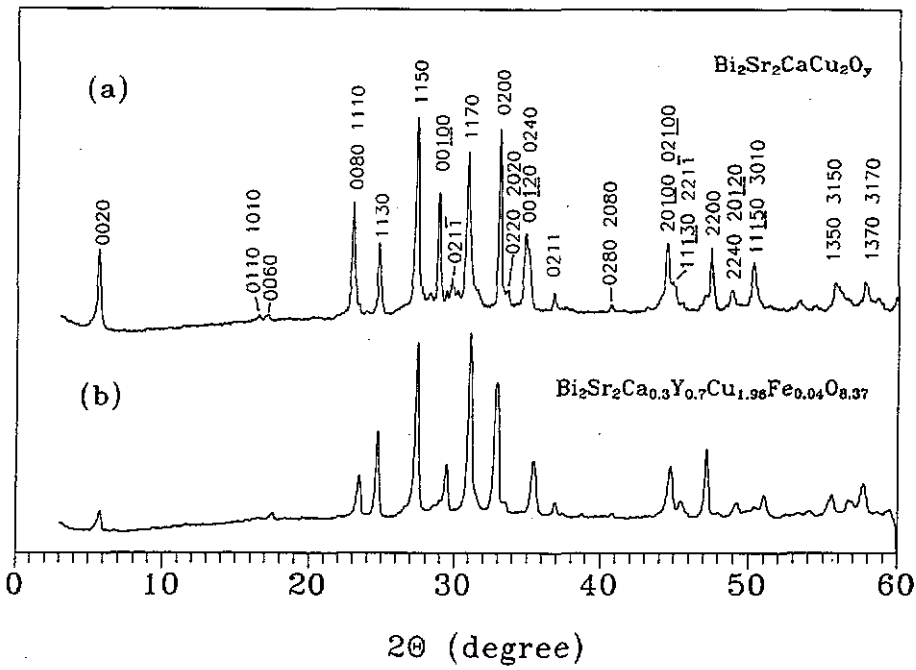

Figure 1. X-ray diffraction patterns for (*a*) $Bi_2Sr_2CaCu_2O_y$ and (*b*) B2:2:1:2YF.

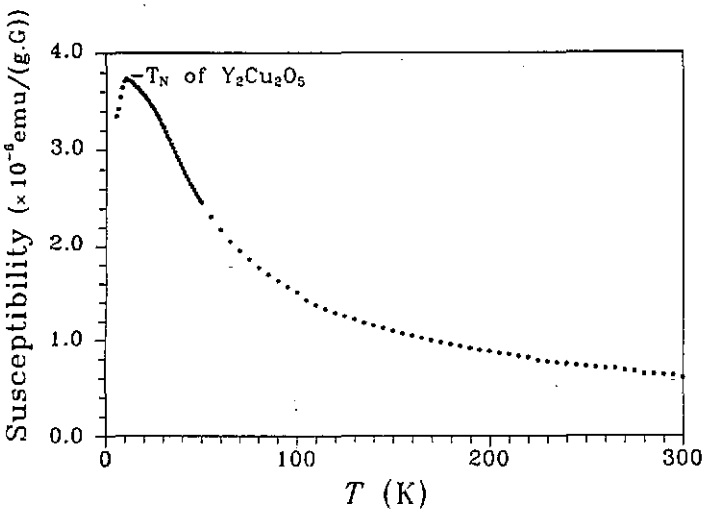

Figure 2. Temperature-dependent magnetic susceptibility for B2:2:1:2YF.

quadrupole doublets (indicated by broken curves). The Mössbauer parameters of doublets 1 and 2 are determined as follows: isomer shift $\delta = 0.65$ mm s^{-1} and 0.21 mm s^{-1}, quadrupole splitting $\Delta Q = 0.96$ mm s^{-1} and 1.07 mm s^{-1}, full width at half-maximum $\Delta\Gamma = 0.37$ mm s^{-1} and 0.82 mm s^{-1} and fractional absorption area $A = 6\%$ and 94%, respectively. Because the Fe atoms can also substitute for Cu atoms in the minor phase $Y_2Cu_2O_5$ in the sample, doublet 1 with the much larger δ-value may arise from the contribution of this impurity. Doublet 2 with a larger A-value should be attributed to the

Table 2. The average oxygen content and Néel temperatures for $Bi_2Sr_2Ca_{0.3}Y_{0.7}Cu_{1.96}Fe_{0.04}O_y$ vacuum annealed at different temperatures.

Annealing temperature (°C)	Average oxygen content y	T_N (±5 K)
Non-annealed	8.51	55
400	8.40	180
600	8.38	>300

contribution of the main phase B2:2:1:2YF. Its $\Delta\Gamma$, which is much larger than the natural linewidth of ^{57}Fe (about 0.23 mm s^{-1}), results from a distribution of quadrupole splittings mainly due to the modulation structure in the B2:2:1:2YF phase.

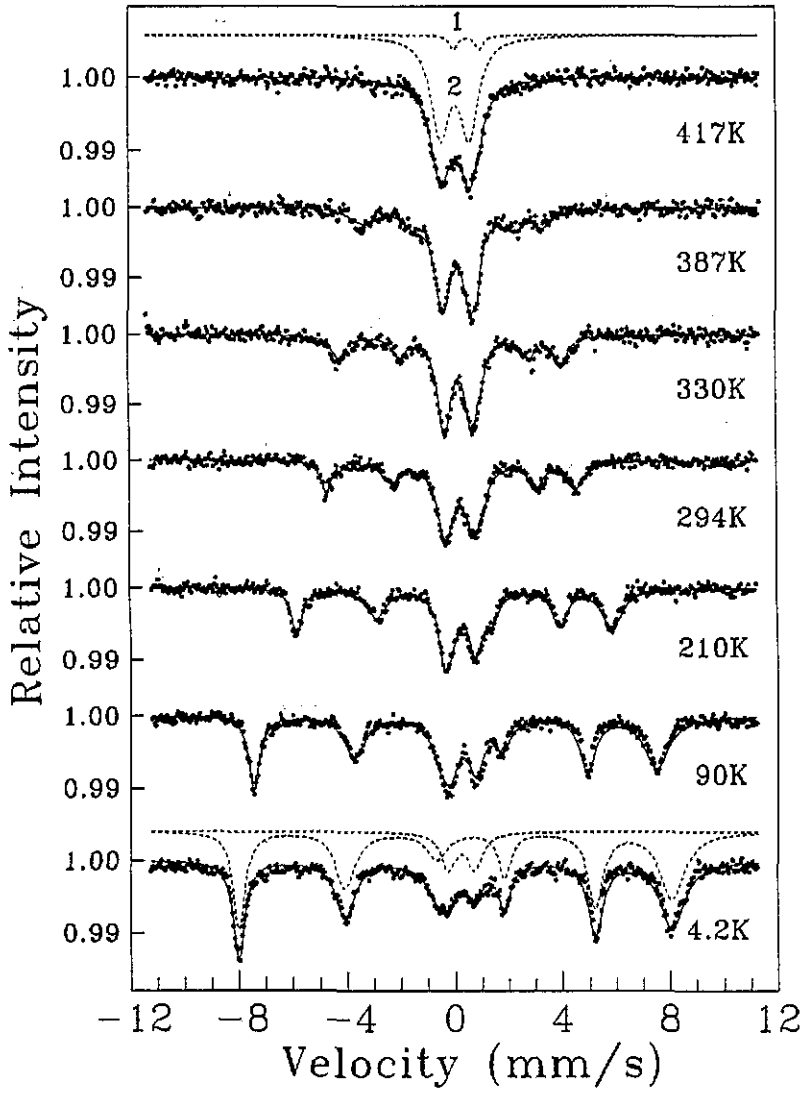

Figure 3. Representative Mössbauer spectra for B2:2:1:2YF at various temperatures.

In comparison with the Mössbauer spectrum at 417 K, the spectra at temperatures below 417 K have extra absorption lines as shown in figure 3. These lines are due to the magnetic hyperfine splitting and imply the presence of magnetic ordering in the sample. The positions and intensities of the magnetic splitting lines on either outer side of the quadrupole-splitting pattern are asymmetric here. Therefore we fit these spectra with a superposition of one mixed magnetic–quadrupole hyperfine subspectrum and one quadrupole doublet. To reduce the number of fitting parameters, the small contribution from $Y_2Cu_2O_5$ is neglected. Both typical subspectra are shown in the spectrum at 4.2 K in figure 3 (indicated by broken curves). The sextet is the mixed magnetic–quadrupole hyperfine subspectrum. The determined effective hyperfine field H, quadrupole splittings ΔQ ($\equiv \frac{1}{2}eQV_{zz}(1+\frac{1}{3}\eta^2/3)^{1/2}$), isomer shifts δ and fractional absorption area A for the sextet and doublet from 4.2 to 407 K are listed in table 3. The hyperfine parameters for the sextet are determined by the positions and relative absorption area ratios of the magnetic splitting lines and the related theoretical formulations can be found in [13]. The angles θ and φ specifying the direction of H with respect to the principal axis of the electric field gradient, and the asymmetric factor η are not presented in table 3 because the spectra can be fitted by wide ranges of these parameters. Fortunately, the values of H, ΔQ, δ and A determined are insensitive to the various values of θ, φ and η. The value of T_N, defined as the temperature at which the magnetically split lines are unresolved and simultaneously the fitted value of H will be zero, is estimated to be 412 ± 5 K. From figure 3 and table 3, we find that the area of the doublet decreases as the temperature is decreased, while the area of the sextet increases at the expense of the area of the doublet. This indicates that some regions in the sample are still in a paramagnetic state below 417 K and the percentage of these regions decreases as the temperature is decreased. Such a phenomenon was also found in the temperature-dependent Mössbauer effect of $La_2Cu_{0.9945}Fe_{0.0055}O_4$ and was thought to arise from a distribution of Néel temperatures due to the inhomogeneity of the oxygen content in the sample [8]. In our sample, the oxygen content is non-stoichiometric and the measured value of T_N is also sensitive to its average oxygen content (see table 2). Thus the regions with different oxygen contents in the sample should have different magnetic ordering temperatures and intensities of the hyperfine field at the Fe nuclei which are related to the magnetization in the region. From table 3, it can be seen that the change in the fractional absorption area A of the doublet below 150 K is relatively small. This indicates that the Néel temperatures are distributed mainly in the range $150\ \text{K} \lesssim T \lesssim 417$ K and about 15% of the B2:2:1:2YF sample is still in a paramagnetic state at 4.2 K. Here the effective hyperfine field H determined by our fitting method will be very close to the most probable value in the distribution of hyperfine field intensities at Fe nuclei. The single Néel temperature T_N is related only to these $H(T)$ data. From the spectra at low temperatures, we find that the widths of the magnetically split lines are apparently asymmetric. For example, the linewidths of the sextet at 4.2 K are as follows: $\Delta\Gamma_1 = 0.53$ mm s^{-1}, $\Delta\Gamma_2 = 0.87$ mm s^{-1}, $\Delta\Gamma_3 = 0.91$ mm s^{-1}, $\Delta\Gamma_4 = 0.55$ mm s^{-1}, $\Delta\Gamma_5 = 0.65$ mm s^{-1} and $\Delta\Gamma_6 = 1.09$ mm s^{-1} (the lines are numbered from the negative velocity). Lines 1, 4 and 5 of this sextet are much narrower than lines 2, 3 and 6. This implies that there is also a correlation between the distributions of the hyperfine fields and quadrupole splittings [14, 15]. In B2:2:1:2YF, such a correlation may result from the non-cubic environments (owing to the modulation structure of the sample) around the iron atoms which induce various non-spherical distributions of the electrons surrounding iron nuclei. These electrons can simultaneously contribute a magnetic dipolar field and an electric field gradient at the Fe nucleus, and both of them are dependent on the distribution of the electrons.

The normalized magnetic hyperfine field $H(T)/H(0)$ of Fe nuclei in B2:2:1:2YF as

Table 3. Some Mössbauer parameters for the B2:2:1:2YF sample at various temperatures.

	Sextet			Doublet		
T (K)	H (kOe)	ΔQ (mm s^{-1})	δ (mm s^{-1})	$\lvert\Delta Q\rvert$ (mm s^{-1})	δ (mm s^{-1})	A (%)
4.2	499	−0.54	0.41	0.98	0.34	15
20	497	−0.57	0.41	1.01	0.38	22
40	492	−0.58	0.44	0.96	0.43	24
60	483	−0.56	0.43	0.98	0.42	26
90	464	−0.58	0.42	0.97	0.42	26
120	443	−0.55	0.41	1.01	0.40	28
150	418	−0.53	0.39	0.99	0.40	26
180	391	−0.54	0.37	0.95	0.42	32
210	364	−0.52	0.37	0.99	0.41	37
240	337	−0.49	0.31	0.99	0.40	39
270	310	−0.49	0.36	0.99	0.36	46
294	288	−0.46	0.23	1.01	0.33	51
296	285	−0.47	0.29	1.03	0.30	47
330	257	−0.54	0.27	1.02	0.31	60
360	233	−0.45	0.28	1.04	0.28	72
387	213	−0.62	0.32	1.05	0.25	66
397	200	−0.55	0.27	1.08	0.23	75
407	176	−0.65	0.36	1.05	0.28	79

a function of temperature is plotted in figure 4. Here $H(0)$ is assumed to be equal to $H(4.2\ \mathrm{K})$ and the hyperfine field at Fe nuclei is assumed to be proportional to the Cu sublattice magnetization. It can be seen from figure 4 that the temperature dependence of $H(T)/H(0)$ for B2:2:1:2YF behaves like that for $La_2Cu_{0.9945}Fe_{0.0055}O_4$ also observed by ^{57}Fe Mössbauer spectroscopy [8]. Tang *et al* [8] described their data via the thermal excitation of spin waves in a highly anisotropic 3D antiferromagnetic model proposed by Singh *et al* [16]. Here we use the same theoretical model to fit our $H(T)/H(0)$ data. According to the expression for the reduction $\delta M(T)$ in sublattice magnetization in [16], we can write the following equation:

$$\frac{H(T)}{H(0)} = \frac{M(T)}{M(0)} = 1 - \frac{2}{\pi^2}\frac{k_B T}{JM(0)}\int_0^{\pi} \mathrm{d}\theta_z \ln\left[1 - \exp\left(-\frac{2J\gamma}{k_B T}(1-\cos\theta_z)^{1/2}\right)\right]^{-1}$$

where $M(0)$ multiplied by $g\mu_B$ is the true magnetization per atom at zero temperature, J is the intra-planar exchange energy and γ is the ratio of effective inter-planar to intra-planar hopping strength. The theoretical curve (the full curve in figure 4) can fit the data well and the parameters J and γ are determined to be $1364/M(0)$ K and $0.008M(0)$, respectively. For B2:2:1:2YF sample, the average Cu valence, corresponding to the oxygen content $y = 8.37$, is about +2.02. Therefore we assume that $M(0) = 0.5$ for the Cu sublattice and then obtain $J = 2728$ K and $\gamma = 0.004$. The value of J is higher while the value of γ is lower than those for $La_2Cu_{0.9945}Fe_{0.0055}O_4$ ($J = 1600$ K and $\gamma = 0.011$ for the latter). In this model, $H(T)/H(0)$ (or $M(T)/M(0)$) will be proportional to T^2 characteristic of a 3D system for $k_B T \ll 2J\gamma$ and proportional to $T \ln T$ characteristic of a quasi-2D system for $k_B T \gg 2J\gamma$[16]. Here $2J\gamma$ is determined to be about 22 K which is the characteristic temperature at which a 3D-to-2D crossover occurs. It should be noted that there are two kinds of distance between CuO_2 planes in B2:2:1:2YF (the distances between CuO_2 planes in La_2CuO_4 are equal). Therefore the model proposed by Singh *et al*, which considers only one kind of inter-planar coupling, should be viewed as an approximate model for

B2:2:1:2YF. Rosov [17] suggested an alternative explanation for the data obtained by Tang *et al.* He argued that, because the temperature dependence of the sublattice magnetization for La_2CuO_4 observed by neutron diffraction measurements [4] nearly follows a spin-$\frac{1}{2}$ mean-field magnetization curve, the anomalous behaviour of $H(T)/H(0)$ in $La_2Cu_{0.9945}Fe_{0.0055}O_4$ should be attributed to the influence of Fe magnetic impurities, i.e. the behaviour can be explained by a modified mean-field theory [18] considering the difference between the probe impurity and host spins and the different host–host and host–impurity moment couplings. In the following, we also use the modified mean-field theory to fit the data on $H(T)/H(0)$ for B2:2:1:2YF. On the basis of the equation derived by Jaccarino *et al* [18], one takes $H(T)/H(0) = B_S(y)$ and $B_S(y)$ is the Brillouin function, $y = (\zeta T_N/T)M_h(T)/M_h(0)$ and $\zeta = g\mu_B S H_0^{Fe-Cu}/k_B T_N$. Here $g\mu_B S$ is the Fe magnetic moment, S is the Fe spin, T_N the ordering temperature, H_0^{Fe-Cu} the Fe–Cu exchange field at zero temperature and $M_h(T)/M_h(0)$ the normalized host magnetization. Assuming that $M_h(T)/M_h(0)$ fits the spin-$\frac{1}{2}$ mean-field magnetization curve and $T_N = 412$ K, we choose three Fe spin values $S = \frac{3}{2}$, 2 and $\frac{5}{2}$ and adjust ζ-values to fit the $H(T)/H(0)$ data for different Fe spins. The three theoretical curves with different Fe spins and fitted parameters are close to each other. Therefore only the curve with $S = \frac{5}{2}$ and $\zeta = 1.42$ is plotted in figure 4 as a broken curve (short dashes). It is clearly seen from this figure that the anisotropic 3D antiferromagnetic model can explain the magnetization behaviour of B2:2:1:2YF much better than the modified mean-field theory can. Thus we believe that the magnetic behaviour of non-superconducting $Bi_2Sr_2Ca_{0.3}Y_{0.7}Cu_{1.96}Fe_{0.04}O_y$ is also like that of a highly anisotropic 3D antiferromagnet, but the discrepancy between $M(T)/M(0)$ in $La_2Cu_{0.9945}Fe_{0.0055}O_4$ observed by neutron scattering [4, 17] and that observed by other local probes such as NQR [7], μSR [2, 19] and Mössbauer spectroscopy [8] remains unexplained.

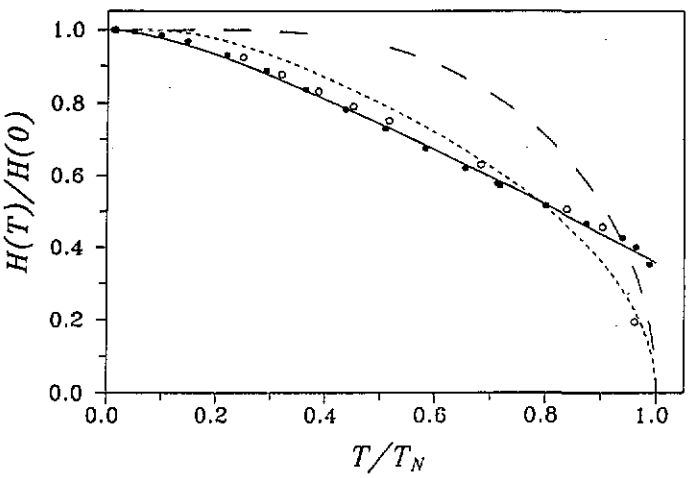

Figure 4. Normalized magnetic hyperfine field $H(T)/H(0)$ of Fe nuclei in B2:2:1:2YF as a function of temperature (●) where $H(0)$ is assumed to be equal to $H(4.2\ K)$: ——, the theoretical curve calculated using a highly anisotropic 3D antiferromagnetic model; - - - -, theoretical curve calculated using a modified mean-field theory; – – –, spin-$\frac{1}{2}$ mean-field magnetization curve; ○, data for $La_2Cu_{0.9945}Fe_{0.0055}O_4$ (from [8]).

4. Conclusion

We have found that oxygen desorption takes place slowly in the as-prepared $Bi_2Sr_2Ca_{0.3}Y_{0.7}Cu_{1.96}Fe_{0.04}O_y$ sample and the value of the Néel temperature T_N is closely related to the oxygen content. The temperature dependence of the magnetic hyperfine field

at Fe nuclei determined by Mössbauer effect measurements can be explained quite well by the anisotropic 3D antiferromagnetic model proposed by Singh *et al.* The intra-planar exchange energy J and the ratio of γ effective inter-planar to intra-planar hopping strength are determined to be 2728 K and 0.004, respectively, for the Cu sublattice.

Acknowledgment

We are indebted to the National Science Council of the Republic of China for financial support of this work.

References

[1] Le L P, Luke G M, Sternlieb B J, Uemura Y J, Brewer J H, Riseman T M, Johnston D C, Miller L L, Hidaka Y and Murakami H 1990 *Hyperfine Interact.* **63** 279
[2] Uemura Y J, Kossler W J, Yu X H, Kempton J R, Schone H E, Opie D, Stronach C E, Johnston D C, Alvarez M S and Goshorn D P 1987 *Phys. Rev. Lett.* **59** 1045
[3] Nishida N, Miyatake H, Shimada D, Okuma S, Ishikawa M, Takabatake T, Nakazawa Y, Kuno Y, Keitel R, Bewer J H, Riseman T M, Williams D L, Watanabe Y, Yamazaki T, Nishiyama K, Nagamine K, Ansaldo E J and Torikai E 1988 *J. Phys. Soc. Japan* **57** 597
[4] Yamada K, Kuno E, Endoh Y, Hidaka Y, Oda M, Suzuki M and Murakami T 1987 *Solid State Commun.* **64** 753
[5] Tranquada J M, Cox D E, Kunnmann W, Moudden H, Shirane G, Suenaga M, Zolliker P, Vaknin D, Sinha S K, Alvarez M S, Jacobson A J and Johnston D C 1988 *Phys. Rev. Lett.* **60** 156
[6] Rossat-Mignod J, Boucherle J X, Burlet P, Henry J Y, Jurgens J M, Lapertot G, Regnault L P and Schweizer J 1990 *Proc. Int. Semin. on High Temperature Superconductivity* ed V L Aksenov, N N Bogolubov and N M Plakida (Singapore: World Scientific)
[7] Doroshev V D, Krivoruchko V N, Savosta M M, Shestakov A A and Yablonskii D A 1992 *Zh. Eksp. Teor. Fiz.* **101** 190; (Engl. Transl. 1992 *Sov. Phys.–JETP* **74** 102
[8] Tang H, Xiao G, Singh A, Tešanovíc Z, Chien C L and Walker J L 1990 *J. Appl. Phys.* **67** 4518
[9] Lyubutin I S, Terziev V G, Dmitrieva T V and Nasu S 1992 *Hyperfine Interact.* **70** 1203
[10] Nowik I, Kowitt M, Felner I and Bauminger E R 1988 *Phys. Rev.* B **38** 6677
[11] Tamegai T, Koga K, Suzuki K, Ichihara M, Sakai F and Iye Y 1989 *Japan. J. Appl. Phys.* **28** L112
[12] Nishida N, Miyatake H, Okuma S, Tamegai T, Iye Y, Yoshizaki R, Nishiyama K and Nagamine K 1988 *Physica* C **156** 625
[13] Kündig W 1967 *Nucl. Instrum. Methods* **48** 219
[14] Window B 1974 *J. Phys. F: Met. Phys.* **4** 329
[15] Buschow K H J, Czjzek G, Bornemann H-J and Kmiec R 1989 *Solid State Commun.* **71** 759
[16] Singh A, Tešanovíc Z, Tang H, Xiao G, Chien C L and Walker J C 1990 *Phys. Rev. Lett.* **64** 2571
[17] Rosov N 1991 *Phys. Rev. Lett.* **67** 1938
[18] Jaccarino V, Walker L R and Wertheim G K 1964 *Phys. Rev. Lett.* **13** 752
[19] Singh A, Tešanovíc Z, Tang H, Xiao G, Chien C L and Walker J C 1991 *Phys. Rev. Lett.* **67** 1939